INTERPRETATION OF POLARIZATION RESPONSES OF URBAN AREA

Kang, Moon-Kyung[1*], Yoon, Wang-Jung[2], Kim, Kwang-Eun[3], Choi, Hyun-Seok[4]

[1*] Chonnam National University, heidiyaa@lycos.co.kr
[2] Chonnam National University, wjyoon@chonnam.ac.kr
[3] Korea Institute of Geoscience & Mineral Resources, kimke@kigam.re.kr
[4] Chonnam National University, ggumikni@nate.com

ABSTRACT:

Polarization of the radar wave refers to the ellipticity angle and orientation angle of the polarization ellipse. An evaluation of the polarization response can help understand the scattering mechanisms involved for a particular area of interest or provide information for image classification and algorithm section.

C- and L-band polarization responses measured at urban area show the results that the polarization behavior for dihedral corner reflector or short, thin cylinder reflector appears at located in city streets or buildings site which are lined up and the polarization behavior for a large conducting sphere appears at parts of test site particularly river, flat, and vegetated areas. Also, the co- and cross-polarized response graphs and polarimetric parameters are discussed.

KEY WORDS: SAR, SAR polarimetry, SIR-C, polarization response

1. INTRODUCTION

The use of active microwave and millimetre wave technology in remote sensing is an established practice. In the beginning, the need for using the polarimetric properties of electromagnetic waves were not understood, but in recent years it has been recognized that polarimetry is essential in determining certain target features and in separating targets from clutter.

Complete understanding of radar polarimetry requires a knowledge of both single-frequency electromagnetic waves, the completely polarized case, and waves that span a finite frequency spectrum, the partially-polarized case. It is essential to consider the vector nature of waves, how they are transmitted and received by an antenna, and how their interaction with a target is described. It is often helpful to represent polarizations graphically. A straightforward means of classifying terrain is by plotting the radar cross section of the resolution cell as a function of the antenna polarization state and comparing it to a similar plot for a known target [1].

A three-dimensional plot of the cross section as a function of tilt and ellipticity angles has been called the polarization signature or the polarization response of the target. Three dimensional polarization signature graphs are commonly used in the literature to illustrate the polarimetric properties of terrain elements [2]. These graphs display the properties of co- or cross-polarized polarimetric radar returns as they are distributed over half of Poincare sphere (they are ambiguous in the handedness of elliptical polarizations). In general, the signatures should show systematic variation with incident angle for specific material types and should identify preferred polarization states for material classification where these exist [1].

As our knowledge of radar polarimetry grows the number of applications and usefulness of the data will also grow. In this paper, we discuss the application of polarization responses in polarimetry techniques to understand the scattering mechanisms involved for a particular area of interest. The objective of this work is to provide a physically based interpretation of observed polarimetric radar responses of urban area.

2. IMAGE DATA AND PROCESSING

2.1 SIR-C Image Data

The SAR data analyzed in this work are multi-look complex (MLC) images acquired by the fully polarized SIR-C system over Seoul and Gyunggi-do (Korea) on April 12, 1994. SIR-C acquisition mode was fully polarimetric at C- (5.304 ㎓) and L- (1.254 ㎓) band and the orbit direction was descending. Table 1 presents a summary of the SIR-C image data characteristics.

Table 1. Summary of the SIR-C image data set

Latitude at image center	37.4513664
Longitude at image center	127.3009644
Processed scene range (km)	24.5875015
Processed scene azimuth (km)	99.9375076
Incidence angle	39.018
Radar wavelength (cm)	5.8 (C-band), 23.5 (L-band)
Polarization	HH, HV, VV
Line spacing (m)	12.50
Pixel spacing (m)	12.50

2.2 Image Processing

As shown in Figure 1, SIR-C image data were synthesized HH, VV, HV polarizations, and total power (TP) images from SIR-C compressed scattering matrix. And then the HH, VV, and HV polarization images as red, green, blue were composite each C- and L-band, respectively. RGB composite images were classified to 10 classes by unsupervised classification using K-means method, and applied majority analysis to classification images in the 3×3 kernel size. Each classification images were converted into vector layers from selected classification classes. Converted vector layers were exported to region of interest (ROI) for extracting polarization responses. The test site is located in Sungdong-gu area of the Seoul (Korea) as shown in Figure 2.

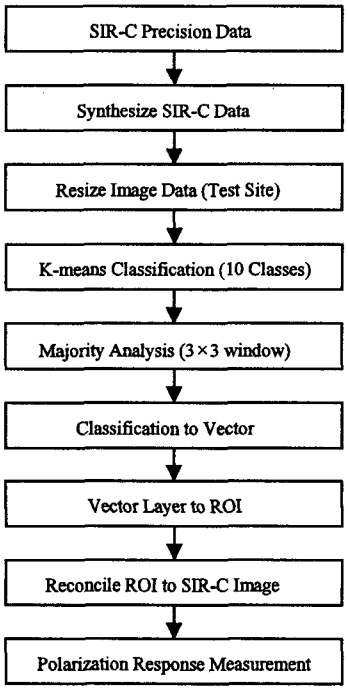

Figure 1. Flow chart of image processing.

3. RESULTS

3.1 SAR Image Texture

SAR image texture analysis may provide additional information for a better discrimination of polarimetric properties of surface elements. Figure 2 displays the imagery of RGB color composites of three polarimetric channels HH (R), VV (G), HV (B), and each polarimetric gray scale image for C- and L-band.

Flat surfaces that reflect little or no microwave energy back towards the radar will always appear dark in radar images. When city streets or buildings are lined up in such a way that the incoming radar pulses are able to bounce off the streets and then bounce again off the buildings (called a double-bounce) and directly back towards the radar they appear very bright in radar images. Roads and freeways are flat surfaces so they appear dark. Buildings which were not lined up so that the radar pulses are reflected straight back will appear light grey, like very rough surface. For RGB color composite images, red, green, and blue color areas appear at regions observed HH, VV, and HV polarizations strongly.

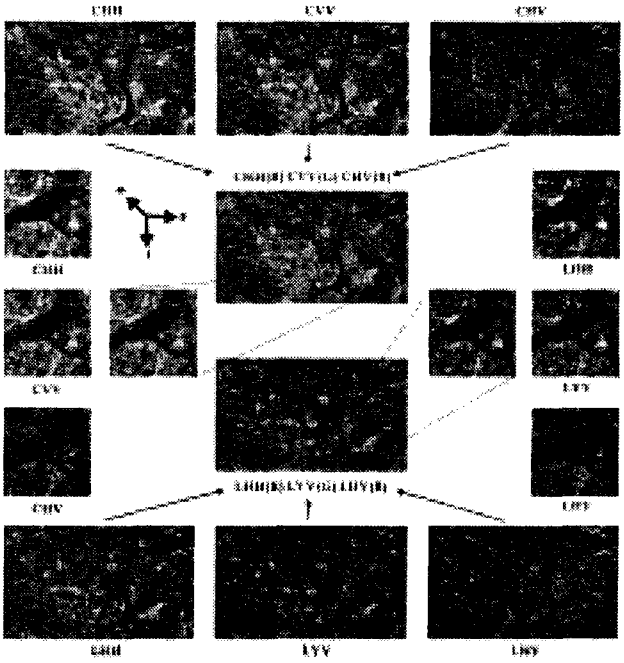

Figure 2. RGB color composite images of C- and L-band with HH (R), VV (G), HV (B) polarization, respectively. The red box area is test site for measurement of polarization response.

3.2 Polarization Response Graphs

C- and L-band polarization responses measured according to 10 classes of image classification show the results that the polarization behavior for large conducting sphere and the polarization behavior for a dihedral corner reflector or a short, thin cylinder reflector.

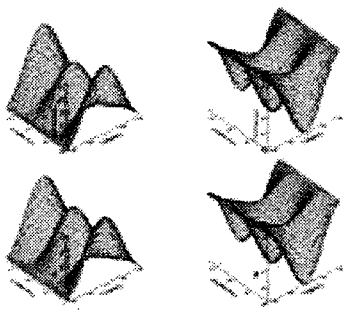

Figure 3. Co-polarized (1st column) and cross-polarized (2nd column) responses graphs at river area mainly (1st row: C-band, class 1; 2nd row: L-band, class 2).

Figure 3 displays co- and cross-polarized graphs in class 1 at C-band and in class 2 at L-band presumed at river, river basin, and bare soil area primarily (refer to Figure 6). The results of these areas show the polarization behavior of large conducting spheres or flat surfaces characteristics. For a large conducting sphere, the co-polarized response shows that the maximum measured scattering cross section occurs for linear polarization and the scattering cross section is independent of the linear polarization orientation angle. For the cross-polarized response, the measured scattering cross section is greatest for the circular polarizations and smallest for linear polarizations. A large flat surface at normal incidence would have the same polarization as a large sphere [2].

Figure 4 displays the measured co- and cross-polarized responses for C- and L-band according to image classification results using K-means. The polarization characteristics of the test site show the behavior for the dihedral corner reflector in class 9 and 10 at C-band and class 10 at L-band, because of double reflections from ground to buildings and back to the radar. Figure 6 shows the land cover classification map that was supplied by the Ministry of Environment Republic of Korea (MOE) overlaid the image classification results. Two images (second row) are the results overlaid the class 10 at C- and L-band. These areas are located in city streets or buildings which are lined up.

In general, a wave scattered from a dihedral corner reflector will undergo a reflection at each surface and return in the direction from which it came. The co- and cross-polarized responses of the dihedral corner reflector are very different from those of the sphere. The co-polarized response possesses two minima at linear polarizations offset by ±45° from the horizontal and vertical polarizations, and the cross-polarized response has maxima at these locations. For the cylinder oriented, the maximum in the co-polarized response and one of the minima in the cross-polarized response occur at the linear polarization with the same orientation as the cylinder. Both the co-polarized and cross-polarized responses also have minima at the linear polarization orthogonal to the cylinder orientation [2].

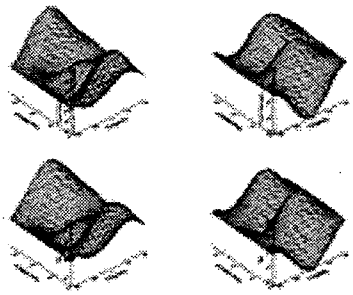

Figure 4. Co-polarized (1st column) and cross-polarized (2nd column) responses graphs at buildings area mainly (1st row: C-band, class 10; 2nd row: L-band, class 10).

Figure 5 shows the measured co- and cross-polarized responses in class 5, 6, 7, 8 at C-band and in class 3, 4, 5, 6, 7, 8, 9 at L-band. These classes appeared at flat areas like loads and freeways, buildings areas partly which were not lined up, and vegetated areas. As shown in Figure 5, the polarization characteristics of these areas show the mixed behavior for a dihedral corner reflector and a large conducting sphere.

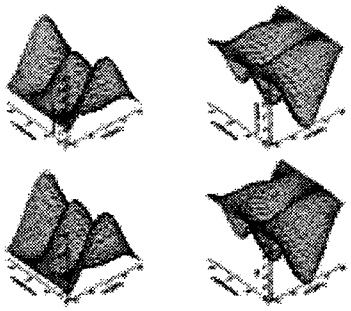

Figure 5. Co-polarized (1st column) and cross-polarized (2nd column) responses graphs at flat, urban partly, and vegetated areas (1st row: C-band, class 5; 2nd row: L-band, class 4).

Figure 6. Land cover classification map overlaid the classes (black area) of SIR-C image classification results using K-means method (1st row: C-band, class 1 (left), L-band, class 2 (right); 2nd row: C-band, class 10 (left), L-band, class 10 (right)).

3.3 Polarimetric Parameters

Table 3 lists the radar backscatter characteristics for the chosen training area. σ°_{HH}, σ°_{VV}, and σ°_{HV} are the SIR-C backscattering coefficients in normalized according to image classification results using K-means method. The first row values are co-polarized, second row values are

cross-polarized, respectively. Table 2 presents the class distribution of each class based upon K-means unsupervised classification results at C- and L-band.

Table 2. Summary report of all classes based upon classification results.

Class	C-band (%)	L-band (%)
Class 1	18.76	0.00
Class 2	12.55	25.62
Class 3	11.98	14.51
Class 4	10.06	15.72
Class 5	7.65	11.55
Class 6	5.54	7.14
Class 7	3.57	4.10
Class 8	2.58	2.28
Class 9	2.32	1.23
Class 10	25.01	17.85

Table 3. σ^{o}_{HH}, σ^{o}_{VV}, and σ^{o}_{HV} are the polarimetric backscattering coefficients in normalized over training.

Class	σ^{o}_{CHH}	σ^{o}_{CVV}	σ^{o}_{CHV}	σ^{o}_{LHH}	σ^{o}_{LVV}	σ^{o}_{LVV}
cls1	1.0000	0.8599	0.0771	-	-	-
	1.9039	1.6871	0.1467	-	-	-
cls2	0.9989	0.8456	0.1738	1.0000	0.9275	0.1060
	2.1560	1.8250	0.3751	1.8843	1.7477	0.1998
cls3	0.9976	0.9686	0.1923	0.9988	0.9080	0.1605
	1.8733	1.8188	0.3611	1.9890	1.8082	0.3196
cls4	0.9987	0.9170	0.2118	0.9993	0.9315	0.1836
	2.0572	1.8885	0.4363	1.9789	1.8446	0.3637
cls5	0.9988	0.9149	0.2234	0.9976	0.9489	0.1769
	2.0227	1.8529	0.4523	1.9656	1.8696	0.3486
cls6	0.9986	0.9189	0.2245	0.9971	0.9575	0.1757
	1.9998	1.8401	0.4495	1.9683	1.8901	0.3467
cls7	0.9990	0.9157	0.2166	0.9963	0.9437	0.1641
	1.9971	1.8305	0.4330	1.9583	1.8550	0.3225
cls8	0.9977	0.8000	0.1833	0.9943	0.9150	0.1535
	2.1136	1.6946	0.3884	1.9851	1.8269	0.3066
cls9	0.9981	0.7943	0.1678	0.9975	0.9232	0.1561
	2.0076	1.5978	0.3374	1.9631	1.8168	0.3072
cls10	0.9988	0.6403	0.0764	0.9991	0.5314	0.0502
	1.9947	1.2787	0.1526	2.0089	1.0685	0.1009

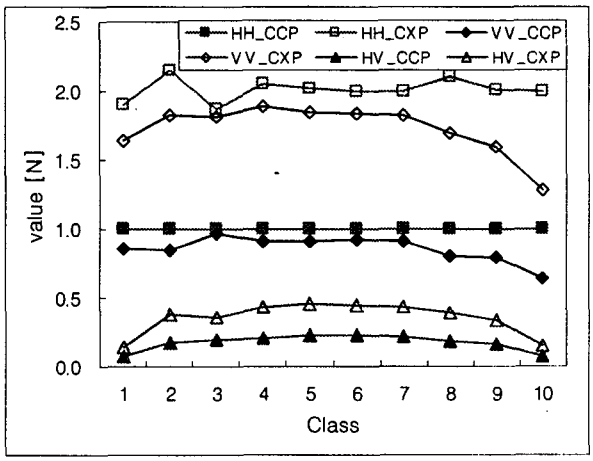

Figure 7. Distribute plot of HH, VV, and HV polarimetric parameters at C-band.

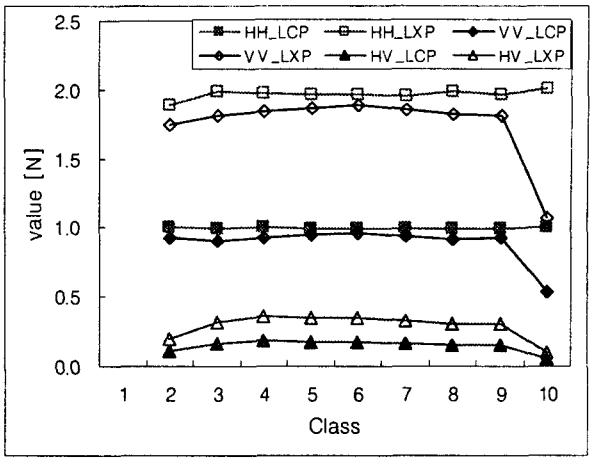

Figure 8. Distribute plot of HH, VV, and HV polarimetric parameters at L-band.

Figure 7 and Figure 8 show the distribute plot of HH, VV, and HV polarimetric parameters at C- and L-band.

4. DISCUSSION

The objective of this study has been to assess the geophysical application of polarimetric SAR data in order to extract relevant information about land surface properties. Results of polarization responses and polarimetric parameters indicate that the dominant scattering property from these fields varies depending on the image classification results by K-means method. From the results described above, we examined that the evaluation of polarization response graphs and related polarimetric parameter are useful for a preliminary research in the case of estimates of land surface properties using simple image classification methods.

References

[1] Henderson, F. M., Lewis, A. J. (eds.), 1998. *Principles & Applications of Imaging Radar.* John Wiley & Sons, NY.

[2] Ulaby, F. T., Elachi, C. (eds.), 1990. *Radar Polarimetry for Geoscience Application.* Artech House, Norwood, MA.